

XMM-Newton CCF Release Note

XMM-CCF-REL-238

An improved model of the RGS effective area based on the build-up of carbon contamination

A.M.T. Pollock

August 23, 2007

1 CCF components

Name of CCF	VALDATE	List of Blocks changed	XSCS flag
RGS1_EFFAREACORR_0005	2001-01-01T00:00:00	EFFAREACORR	NO
RGS2_EFFAREACORR_0005	2001-01-01T00:00:00	EFFAREACORR	NO

2 Changes

Last year saw the introduction of empirical RGS effective area corrections. The original corrections were based on a set of observations of Mkn421 whose spectrum was assumed to be a simple power-law subject to constant galactic absorption. Observations at different times, though of variable intensity and slope, were used to make a polynomial model of the wavelength-dependent changes in effective area, particularly the decrease at long wavelengths that also became clear at the same time. A final comparison with the Crab nebula allowed final adjustments for power-law slope and overall normalisation.

Since then, by comparing the changes observed in the RGS spectra of objects of constant spectrum, it has been shown that the time-variable component of the effective area can be well modelled by a linearly increasing layer of carbon contamination as shown in Fig. 1. This has been combined with a constant polynomial correction and the more detailed model of the Crab spectrum described by Kaastra et al. in a submitted paper that includes additional corrections for dust scattering, pile-up and spatial variations of the spectral index.

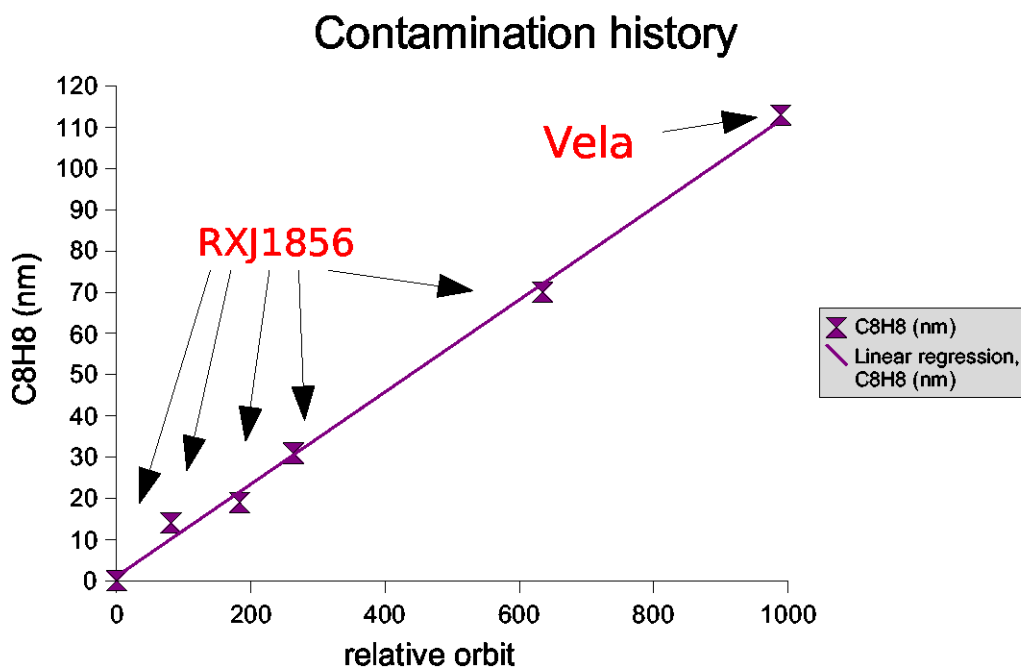
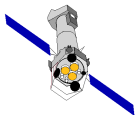
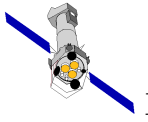


Figure 1: The thickness of the layer of carbon contamination implied by differences in the RGS fluxed spectra of the neutron star RXJ1856-3754 and the Vela Pulsar Wind Nebula, both of which are effectively constant. The linear increase now accounts for the time-variable part of the model of the RGS effective area.



3 Scientific Impact of this Update

This release should contribute to the continuing effort to reconcile the RGS and EPIC instruments.

4 Estimated Scientific Quality

This CCF allows broadband fluxes to be measured at the few percent level but, perhaps more importantly, provides a robust extrapolation into the future of the evolution of the RGS effective area.

5 Test procedures & results

During their construction, many new RGS RMFs have been calculated with these new CCFs including their application to the 11 observations of RXJ1856-3754 throughout the mission shown in Fig. 2. The normalisation of the first order spectra of RGS1 and RGS2 is shown for the following XSPEC model fit jointly to all the first order RGS data only, with the following best-fit parameters with their formal errors.

$$\begin{aligned} \text{TBabs nH} &= 6.1 \times 10^{18} \text{ cm}^{-2} \text{ fixed} \\ \text{bbody kT} &= 62.09 \pm 0.07 \text{ eV} \\ \text{bbody norm} &= 3.162 \pm 0.029 \times 10^{-4} \\ \text{C-statistic} &= 57633.7 \text{ for 54522 PHA bins} \end{aligned}$$

The contamination history shown in Fig 1 is only sensitive to differences in the detected spectrum of RXJ1856-3754 . The good agreement between the RGS black-body temperature and the corresponding independent values of EPIC and *Chandra* demonstrates the reliability of the overall effective area model for which the polynomial correction is particularly important in a spectrum as soft as this.

6 Expected Updates

Routine update are expected on an annual basis as the predictions of the linearly-increasing contamination can be tested.

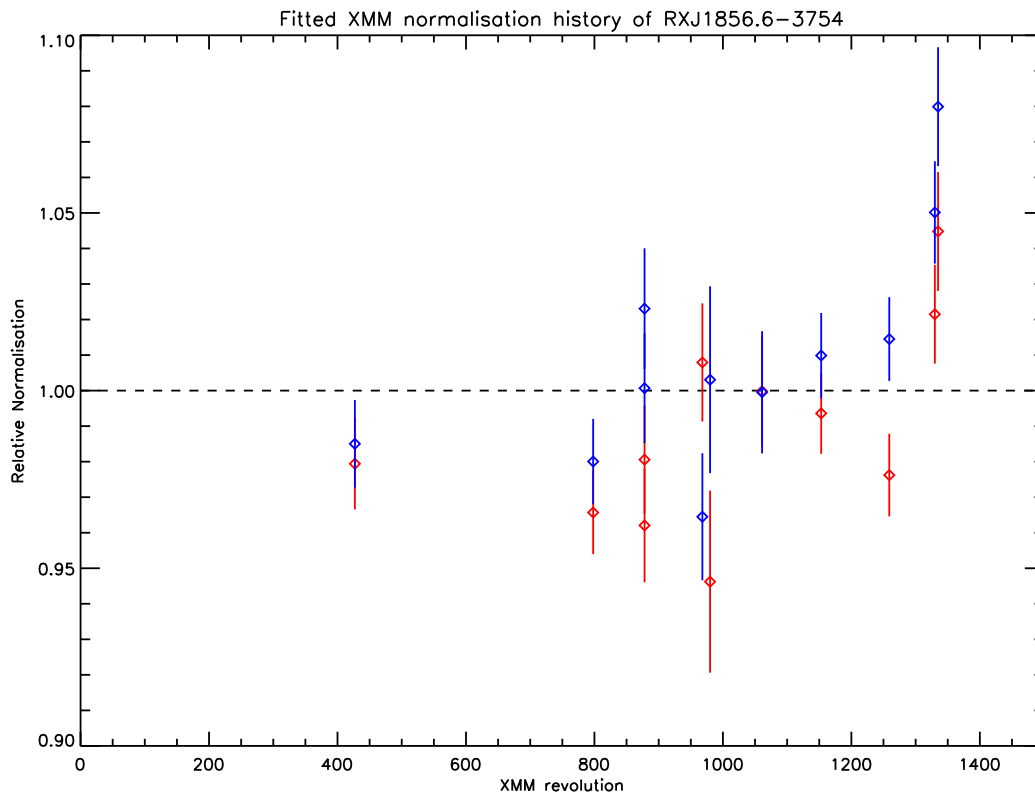
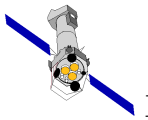


Figure 2: The relative normalisation of RXJ1856-3754 RGS1 (red) and RGS2 (blue) 1st order spectra throughout the mission. All the available data are shown, including the final two observations in rev 1330, which has data problems, and rev 1335, which was an offset pointing.